1996ApJ...463..110T

THE ASTROPHYSICAL JOURNAL, 463:110–119, 1996 May 20
© 1996. The American Astronomical Society. All rights reserved. Printed in U.S.A.

FAR-ULTRAVIOLET SPECTRA OF BROAD ABSORPTION LINE QSOs AND CONSTRAINTS ON MODELS FOR THE IONIZATION STRUCTURE AND METALLICITY OF THE BAL-REGION GAS[1]

DAVID A. TURNSHEK, MICHAEL KOPKO, JR., ERIC MONIER, AND DONETTE NOLL
Department of Physics and Astronomy, University of Pittsburgh, Pittsburgh, PA 15260

BRIAN R. ESPEY
Department of Physics and Astronomy, Johns Hopkins University, Baltimore, MD 21218

AND

RAY J. WEYMANN
Carnegie Observatories, Carnegie Institution of Washington, Pasadena, CA 91101

Received 1995 August 18; accepted 1995 November 17

ABSTRACT

Hubble Space Telescope Faint Object Spectrograph G270H spectra of four moderate- to high-redshift broad absorption line (BAL) QSOs are presented. In addition, evidence is discussed that indicates that the gas that gives rise to the BALs has nonuniform ionization and enhanced abundances. In the context of a photoionization model, ionization parameter fluctuations of at least ~32–16 are needed to explain the observed column densities of different ions of the same element. In such a model, the gas must have very enhanced metal-to-hydrogen abundances relative to solar composition. However, the actual metal-to-hydrogen abundance enhancements are difficult to constrain because they are so model-dependent. For example, in a photoionization model the shape of the photoionizing continuum has a significant influence on the derived metal-to-hydrogen enhancement, but for normally adopted shapes the enhancement is very large, i.e., an enhancement of ~120–230 times solar for nitrogen. If collisional ionization is important, the need for metal-to-hydrogen abundance enhancements would be severely reduced. The derived relative metal abundances are somewhat more robust because the relevant metal-line transitions correspond to similar ionization potentials. In a photoionization model, nitrogen enhancements relative to oxygen and carbon of ~4–3 and 9–10 times solar values, respectively, are indicated. If normal stellar nucleosynthesis is important, the results may be indicative of star formation with a relatively flat initial mass function, with the nitrogen overabundance produced by secondary processing in massive stars. However, large enhancements of elements like phosphorus in some objects suggest that the enrichment scenario may be more complex. In addition, the results discussed here place constraints on the details of a photoionization model for the BAL-region gas. These constraints are unphysical enough that they may indicate that central-source photoionization is not dominant.

Subject headings: quasars: absorption lines — quasars: individual (H0059 − 2735, Q0226 − 1024, H0903 + 1734, Q0932 + 5006, Q1309 − 0536)

1. INTRODUCTION

With the advent of the *Hubble Space Telescope* (*HST*) the broad absorption lines (BALs) present in QSO spectra can now routinely be observed much further down into the UV than was previously the case. We present far-UV spectra of four moderate-redshift BAL QSOs that have been recently observed with the *HST* Faint Object Spectrograph (FOS). We also present an analysis of the first moderate-redshift BAL QSO observed with the *HST* FOS, Q0226 − 1024, the results of which have implications for the ionization structure and elemental abundances of the BAL gas as well as the nature of the ionization model itself. Some reviews and discussions of BAL QSO work, with recent references, can be found in Turnshek (1995, 1988), Weymann (1995), and Turnshek et al. (1994).

Part of the motivation for the work described here is the ability, for the first time, to make reliable measurements of BAL profiles that arise from different ions of the same element for a number of different elements. Korista et al. (1992) presented the first *HST* FOS observations of this type for the BAL QSO Q0226 − 1024, and preliminary observational results on four BAL QSOs more recently observed with the *HST* FOS are presented in § 2. A more thorough analysis of the new data is in preparation. However, the analysis of the Q0226 − 1024 spectrum forms the basis for the results on ionization structure and elemental abundances presented here. The conclusions should equally apply to other BAL regions since Q0226 − 1024 is a representative object.

The approach that we have taken to investigate BAL-region ionization structure and abundances is a general one. For example, in the context of a photoionization model, we have chosen to adopt some simple parameterizations for ionizing continua and then determine what these assumptions imply for ionization stratification and abundances on an element-by-element basis. We believe that this approach is appropriate because some observations suggest that the metal-enrichment scenario may be complex. For example, some objects show evidence of very enhanced phosphorus, and this would have to be accounted for in an enrichment scenario. On the other hand, Korista et al. (1996) have taken an approach that is complementary to our own. They have considered derived BAL-region column densities and a wide range of continuum shapes under the assumption that one of the enrichment scenarios discussed by Hamann & Ferland (1993) is correct. In the context of their assump-

[1] Based on observations with the NASA/ESA *Hubble Space Telescope*, obtained at the Space Telescope Science Institute, which is operated by AURA, Inc., under NASA contract NAS 5-26555.

© American Astronomical Society • Provided by the NASA Astrophysics Data System

1996ApJ...463..110T

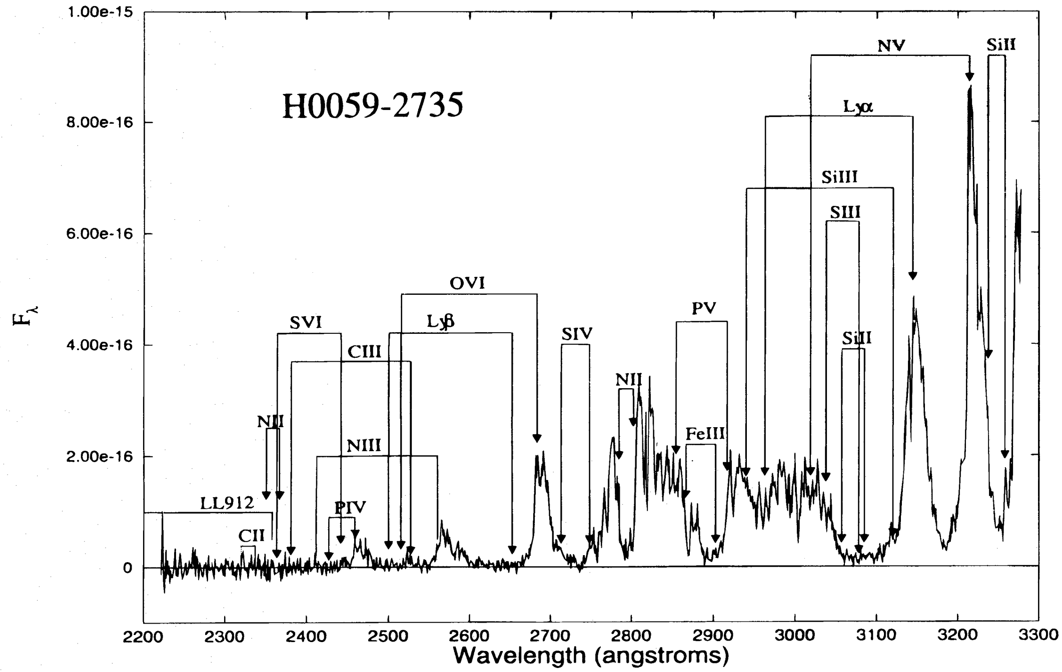

FIG. 1.—*HST* FOS G270H spectrum of the BAL QSO H0059−2735. The labels shown on the spectrum indicate the expected locations of possible BAL troughs.

TABLE 1

JOURNAL OF *HST* FOS G270H[a] OBSERVATIONS

Object	V (mag)	z_{em}	Date	Exposure Time (s)
0059−2735......	17.4	1.60	1994 Jun 28	2502
0903+1734......	17.3	2.76	1995 Mar 26	2262
0932+5006......	17.2	1.92	1993 Apr 21	3228
1309−0536......	17.4	2.22	1994 Jul 12	2502

[a] Spectral resolution $R \approx 1300$.

tions, the question of the minimum required metallicity can be considered, but only if the continuum shape is taken to be unconstrained and a free parameter. We have explicitly not taken this type of approach here, but our results, along with Korista et al.'s results, should help to clarify the problems associated with studies of BAL-region ionization structure, elemental abundances, and the effects associated with an uncertain ionizing continuum shape.

The organization of this paper is then as follows: Techniques for deducing BAL-region column densities and some

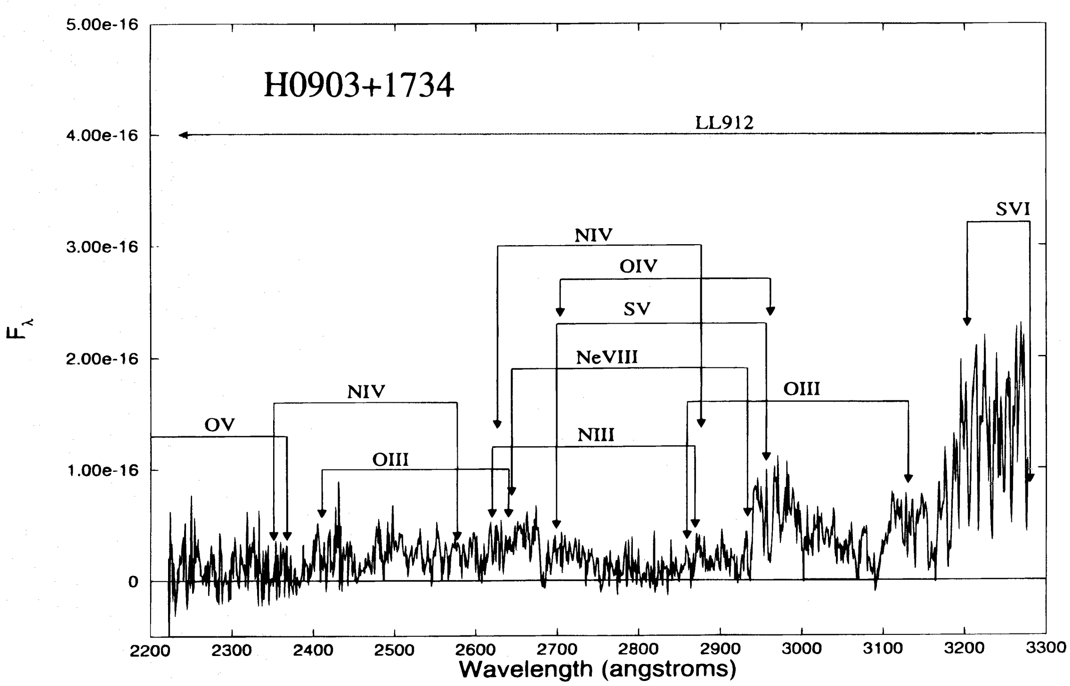

FIG. 2.—Same as Fig. 1, but for the BAL QSO H0903+1734

© American Astronomical Society • Provided by the NASA Astrophysics Data System

1996ApJ...463..110T

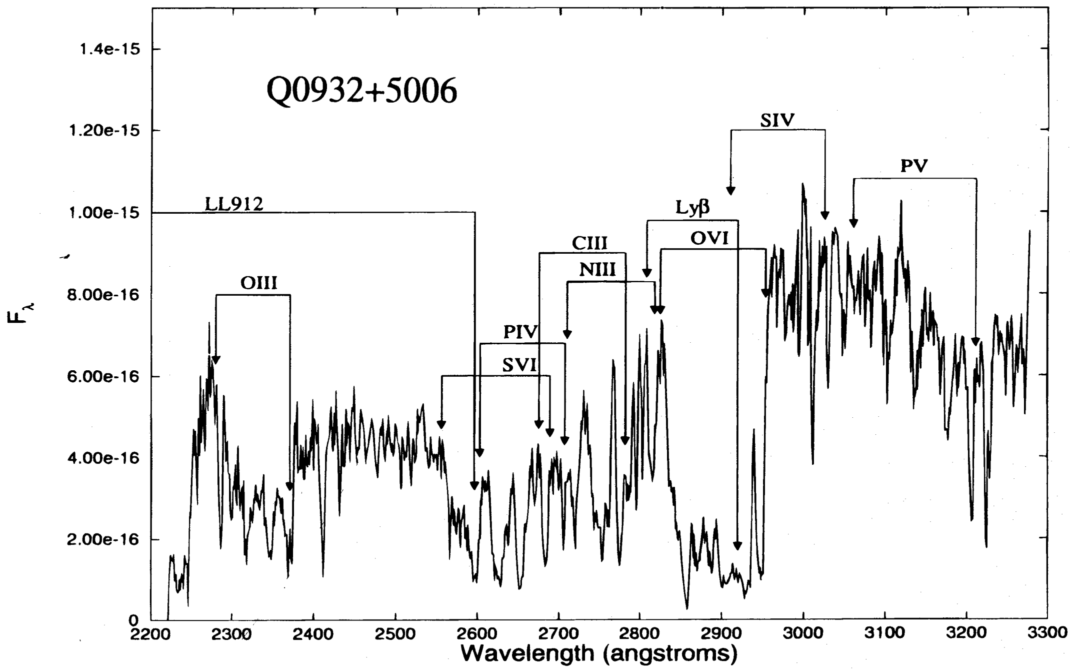

FIG. 3.—Same as Fig. 1, but for the BAL QSO Q0932+5006

relevant observational results from Q0226−1024 are reviewed and discussed in § 3. Constraints on the ionization structure that can be derived by comparing observed column densities to collisional and photoionization models are considered in § 4. The elemental abundances of the BAL gas are considered in § 5. A discussion of some of the implications and the need for future work is given in § 6. A summary is presented in § 7.

2. SOME RECENT *HST* FOS OBSERVATIONS OF BAL QSOs

The journal of *HST* FOS G270H observations for the four recently observed BAL QSOs, along with their magnitudes and redshifts, are presented in Table 1. Figures 1–4 show the spectra of H0059−2735 (Hazard et al. 1987; Wampler, Chugai, & Petitjean 1995), H0903+1734 (Hazard et al. 1984), Q0932+5006 (Turnshek et al. 1984), and Q1309−0536 (Turnshek et al. 1984), respectively. The labels shown on the spectra indicate the expected locations of possible resonance-line absorption troughs as derived from the above references. A thorough analysis of the spectra with the aim of presenting constraints on column densities and column density ratios will be presented elsewhere. However, these spectra and the earlier spectrum of Q0226−1024 presented by Korista et al. (1992) should serve to illustrate the great wealth of information available on different ions of the same element and rarely identified

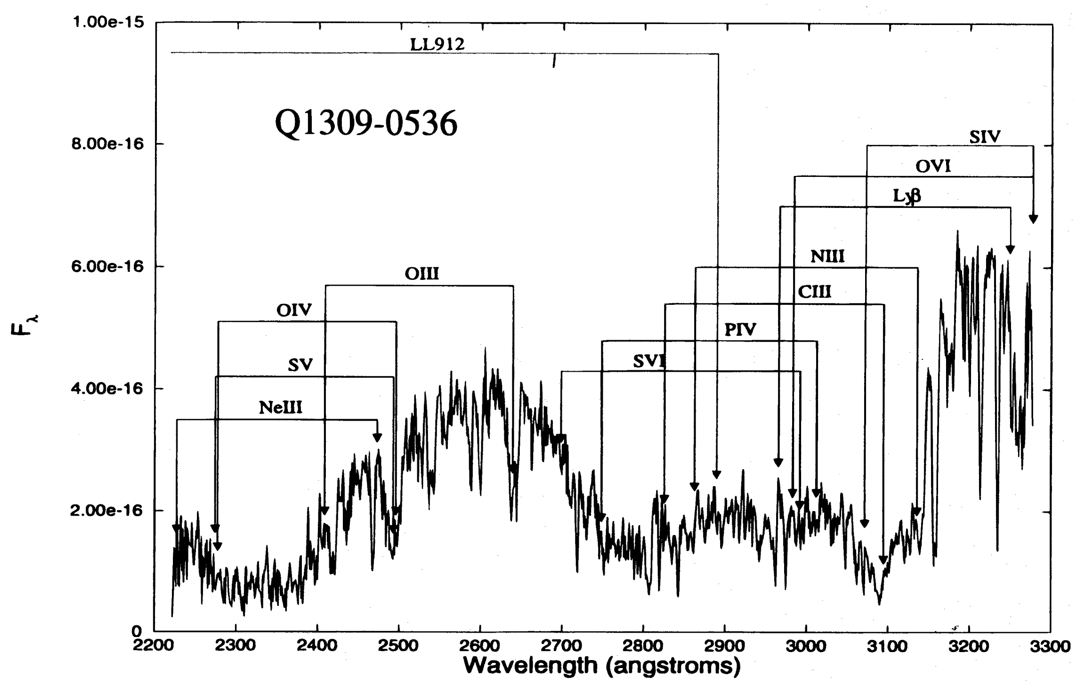

FIG. 4.—Same as Fig. 1, but for the BAL QSO Q1309−0536

© American Astronomical Society • Provided by the NASA Astrophysics Data System

1996ApJ...463..110T

BALs (e.g., P v λλ1117, 1128 or Fe III λ1122) that can be obtained by observing BAL QSOs into the far-UV. Such observations offer a unique way to explore the QSO environment near the central source by studying a region that is expected to be located a few parsecs to a few hundred parsecs from the central source on the basis of photoionization models (Turnshek et al. 1985; Foltz et al. 1987; Turnshek 1988; but see § 6, point 5). Obtaining good data on BAL profiles of different ions of the same element had not been possible until the recent *HST* FOS UV observations of moderate- to high-redshift BAL QSOs. At higher redshifts, where important lines might be observed in the optical, intervening Lyman-limit absorption normally blocks our view of these far-UV lines. In the absence of data on different ions of the same element, the ionization structure cannot be explored without making questionable assumptions. For example, we would have to assume uncertain elemental abundances in the context of some model scenario (e.g., the often adopted solar abundances, results from one of the Hamann & Ferland 1993 evolutionary metal-enrichment grids).

3. BAL-REGION COLUMN DENSITIES

3.1. *Discussion of BAL-Region Column Density Derivations*

To attempt to understand the ionization structure and elemental abundances of the BAL-region gas, we must first have the ability to derive the line-of-sight column densities of ions seen in absorption as a function of outflow velocity. Ideally, we would also like to know how outflow velocity maps into the spatial coordinate along the sight line, but the observations do not normally allow for a model-independent determination of this (but see Turnshek et al. 1988). In particular, we cannot be sure whether the absorption seen at some specific outflow velocity comes from a spatially distinct region (e.g., a cloud or a specific part of an outflowing wind) or from more than one region (e.g., two or more clouds or regions with large spatial separations).

The most straightforward procedures for deriving the line-of-sight column densities as a function of outflow velocity are discussed by Junkkarinen, Burbidge, & Smith (1983), Turnshek (1984b), Grillmair & Turnshek (1987), and Korista et al. (1992). These procedures generally assume that the absorbing material completely and uniformly covers the continuum source, that scattered radiation does not fill in the bottoms of the absorption profiles (violation of this would be a special form of incomplete source coverage), and that the absorption structure is resolved in velocity space (i.e., that absorption in the BAL profile does not become narrower and deeper at higher resolution).

There are several good reasons to believe that the projected area of the BAL region completely covers a region larger than the central continuum source. The central continuum source might have size scales of $\sim 10^{16}$–10^{17} cm from variability considerations, while the region emitting the Lyα broad emission line might be larger than 10^{18} cm in luminous QSOs. Observations of BAL QSOs indicate that the N v BALs must mostly cover the region that is emitting the Lyα broad emission line (Turnshek et al. 1988). In addition, *HST* observations of the "Cloverleaf" BAL QSO H1413+1143 show that the BAL region covers the continuum source and the Lyα broad emission line region along all four sight lines. The similarity of the BAL profiles along the four sight lines indicates that the absorption is likely uniform to within less than $\sim 10\%$ across the central continuum source (Turnshek 1995; Turnshek et al. 1996). The point that the N v BAL region covers the Lyα-emitting region should perhaps be clarified. For example, the models of Ferland et al. (1992) suggest the possibility that the clouds that give rise to Lyα emit very anisotropically and that the sides of the clouds that face the central continuum source are responsible for the bulk of the Lyα emission. Could such a situation be consistent with a model in which the N v BAL region lay closer to the central source than the Lyα broad emission line region, but with the N v BAL region covering the Lyα broad emission line region as seen along our sight line? While this possibility should not be completely dismissed, it still seems somewhat unlikely since, in that case, the projected area of an *inner* N v BAL region would have to be *larger* than the projected effective area of an *outer* Lyα-emitting region and the model would also have to be consistent with the line profiles and redshifts observed for the various broad emission lines.

On the other hand, there appear to be some isolated cases in which the absorption does not completely cover the central continuum source along a single sight line. An Si IV doublet seen in the spectrum of Q0226−1024 (Korista et al. 1992) and a C IV doublet seen in the spectrum of Q1524+517 (Barlow 1995) are examples, and we are aware of at least one other example in an unpublished spectrum. However, there are other BAL doublets that are clearly consistent with complete source coverage. It may be that some of the absorption doublets from clouds that do not cover the continuum source are not true BAL clouds and originate in the inner broad emission line region. Given the normal constraint that the N v BAL region covers the inner Lyα broad emission line region, i.e., a region larger than the central continuum source, such a conclusion would seem to make sense.

Also relevant is the observation that in some of the polarized BAL QSOs the data are consistent with light from the central continuum source being completely covered by the BAL region while extended polarized light scattered from the continuum is not covered (Goodrich & Miller 1995).

With regard to emission from resonance-line scattering filling in the bottoms of absorption troughs, Hamann, Korista, & Morris (1993) have recently considered this by computing some possible resonance line–scattered emission profiles. From the Hamann et al. and earlier work, it is clear that this could be an important effect in some objects at low BAL-region outflow velocity. However, we can always choose to study BAL profiles at high enough outflow velocities to be sure that there is little chance of resonance line–scattered emission filling in the bottoms of the absorption profiles. For example, in their recent study, Wampler et al. (1995) pointed to evidence that suggests that the lowest velocity parts of a BAL profile do not fully cover the region that gives rise to the C IV emission line while the higher velocity parts of the BAL profile fully cover the continuum source (i.e., at higher velocities the central intensities are near zero, indicating moderately high optical depths and complete source coverage). Given the coverage of the Lyα broad emission line region by the N v BAL region, one way the absence of coverage of an emitting region by adjacent absorption could make sense is if the emission were coming from the absorbing clouds. Of course, reliable column densities cannot be obtained in such regions, nor can they be obtained in the saturated regions of BAL troughs, where the

© American Astronomical Society • Provided by the NASA Astrophysics Data System

1996ApJ...463..110T

TABLE 2

BAL Column Densities Deduced from Observations of Q0226−1024

Species	log [N (cm^{-2})]	log (Estimated Error in N)
H^0	15.745	0.05
C^+	< 15.370	0.05
C^{+2}	15.566	0.07
C^{+3}	16.165	0.05
N^+	15.186	0.06
N^{+2}	16.292	0.08
N^{+3}	16.335	0.08
N^{+4}	16.353	0.05
O^{+2}	16.566	0.07
O^{+3}	16.656	0.08
O^{+5}	16.403	0.06
Si^{+3}	15.198	0.05
S^{+3}	14.603	0.06
S^{+5}	15.847	0.07

central intensities are near zero, but these regions are always avoided for the purpose of deriving reliable column densities within the framework of adopted assumptions. A very real concern would be an effect that causes the high-velocity parts of a BAL profile to become weaker not only because the optical depth is dropping but also because the clouds are becoming smaller than the continuum source and not covering it (e.g., Turnshek 1984b raised this possibility). However, template methods for deriving column densities (Grillmair & Turnshek 1987; Korista et al. 1992) usually work so well that it would be surprising if this effect significantly altered the derivation of column densities. Finally, recent Keck HIRES data on a few BAL QSOs (Burbidge 1995; Barlow & Junkkarinen 1994) show that BAL profiles are not resolved into many deeper components at very high resolution.

Taking all of the evidence together, we conclude that the normal methods used to derive column densities, when used with caution, are likely to be generally valid.

3.2. *Some Observational Results*

For the analysis here, the BAL column densities derived from ground-based and *HST* FOS UV spectroscopy of Q0226−1024 will be considered (Korista et al. 1992). The column densities were determined by fitting appropriate templates of column density as a function of velocity to the overlapping BALs (see Korista et al. 1992). The column density results are summarized in Table 2. A somewhat subjective estimate (in the context of our assumptions) of the error in column density is also given in Table 2, based on interactively varying the column density and judging how well it fit the data for the adopted continuum. In some cases, the column densities we adopt are not identical to those reported by Korista et al. (1992), but these differences should be viewed as differences in judgment as to the best-fit values and so to represent uncertainties in some sense. The column density ratios used in the ionization structure analysis of § 4 are somewhat less uncertain than the column densities themselves since, to some degree, they scale similarly with continuum placement for moderate optical depths. All of the fits generally rely heavily on the moderate optical depth parts of the troughs at higher velocity (e.g., outflow velocities of ~10,000–11,000 km s^{-1} provide a good region in Q0226−1024) because in these regions there are fewer worries about saturation or resonance line–scattered radiation filling in the bottoms of the troughs.

4. IONIZATION STRUCTURE

As pointed out earlier, in the absence of data on different ions of the same element, the ionization structure cannot be explored without making additional assumptions (e.g., about elemental abundances). A single-zone collisional ionization model characterized by a single temperature is inadequate for explaining the broad range of observed ionization stages at some outflow velocity. In particular, this is clearly the case for collisional ionization models and for the simple photoionizing continua that will be considered here. While there may be some special continuum shapes that could explain *all* of the column densities (which we assume to be reliable), these continua would be extremely ad hoc. Furthermore, while single-zone photoionization models of the BAL region lead to some relevant constraints on gas density and the location of the BAL region relative to the central source, these models have always been viewed as unreliable for other uses because of the possibility that elemental abundances are very far above and different from solar ratios. As summarized in Table 2, the BAL region of Q0226−1024 provides column density information for different ions of the same element for C (observed C III and C IV BAL profiles and an upper limit on the strength of any C II BAL profile), N (observed N III, N IV, and N V BAL profiles), and O (observed O III, O IV, and O VI BAL profiles). Given the realization that single-zone models are inadequate, we consider constraints that observed column ratios impose on two-zone collisional ionization models (see § 4.1) and two-zone photoionization models (see § 4.2).

Consider the case where we have known column densities $N(X^i)$, $N(X^{i+1})$, and $N(X^{i+2})$ for element X in the i, $i+1$, and $i+2$ stages of ionization, respectively. In a particular outflow velocity interval, a two-zone ionization model implies

$$N(X^i) = n_1(X^i)\Delta r_1 + n_2(X^i)\Delta r_2 \,, \tag{1}$$

$$N(X^{i+1}) = n_1(X^{i+1})\Delta r_1 + n_2(X^{i+1})\Delta r_2 \,, \tag{2}$$

$$N(X^{i+2}) = n_1(X^{i+2})\Delta r_1 + n_2(X^{i+2})\Delta r_2 \,, \tag{3}$$

where n_1 and n_2 are the densities of the appropriate ion in the two zones and Δr_1 and Δr_2 are the thicknesses of the two zones along the sight line. If we define the ratio $R \equiv \Delta r_1/\Delta r_2$, then equations (1)–(3) can be rewritten in terms of column density ratios for an element X in various stages of ionization:

$$\frac{N(X^i)}{N(X^{i+1})} = \frac{n_1(X^i)R + n_2(X^i)}{n_1(X^{i+1})R + n_2(X^{i+1})} \,, \tag{4}$$

$$\frac{N(X^{i+1})}{N(X^{i+2})} = \frac{n_1(X^{i+1})R + n_2(X^{i+1})}{n_1(X^{i+2})R + n_2(X^{i+2})} \,. \tag{5}$$

In general, n_1 and n_2 for the ions of the various elements will be functions of the ionization model, for example, the parameters that describe two-zone collisional or photoionization models. For any one element, there may be a range in parameter space, including a range of R-values, for which the ion column density ratios might match those deduced from the observations. If the acceptable ranges in parameter space for the different elements overlapped one another, it would be an indication that the particular two-zone model being considered was consistent with the observations. Of course, this does not mean that the ionization model is uniquely consistent with the data. However, using this

© American Astronomical Society • Provided by the NASA Astrophysics Data System

1996ApJ...463..110T

approach to estimate the levels of ionization, the abundances of any of the observed elements can be derived in a model-dependent way (see § 5). When considering two-zone models, we will assume that the ions that produce the main observed metal BALs are at or near the dominant stage of ionization for the element in question.

4.1. *Inferences from a Two-Zone Collisional Ionization Model*

To explore the expected column density ratios in a scenario in which the observer's sight line intercepts two collisionally ionized regions that have the same outflow velocity, we used tabulated results on the equilibrium ionization of the elements (Arnaud & Rothenflug 1985; Shull & Van Steenberg 1982). Such a situation might exist if gas densities were high enough relative to the photon density to minimize the effects of central-source photoionization. Shocks caused by collisions between the high-velocity gas components might be involved in heating the gas. However, we generally found that it was not possible to pick two temperatures and a value for R that would simultaneously predict all of the correct ion column density ratios for C, N, and O. Two temperature zones and an R-value that might work well to explain the observed relative ion column density ratios for one element would be significantly discrepant for at least one of the other elements. On the other hand, a model with three ionization zones would, not surprisingly, provide better agreement. In such models, temperatures in the range $\log T \approx 5.0$–5.5 seemed appropriate. For example, to obtain the observed O^{+5}/O^{+3} ratio, $\log T \approx 5.4$ is required and little O^{+2} is present, while the observed O^{+3}/O^{+2} ratio suggests values closer to $\log T \approx 5.1$, but then little O^{+5} is present. By selecting temperatures that are somewhat further apart than these two values, we can obtain agreement in a two-zone model for three ions of this one element, but these values do not then adequately explain the results for C and N. While we have not pursued these models, it should be noted that hydrogen is generally much more highly ionized (see § 5) at these temperatures than in the photoionization models that are considered in § 4.2. This may be relevant to abundance derivations. Given the uncertainties in the global characteristics of any collisional ionization model, it is not clear if collisional ionization could be ruled out on the basis of some other observational result (e.g., expected X-rays, strong line emission from collisional excitation).

4.2. *Inferences from a Two-Zone Photoionization Model*

Photoionization has always been attractive when a strong central continuum source is actually observed, as it is in QSOs. As suggested earlier, though, analysis of the results in Table 2 indicates that, for models that adopt rather simple parameterizations of the ionizing continuum, a single-zone photoionization model is unable to explain the observed column density ratios for three ions of the same element, which indicates that at least a two-zone BAL cloud model is required. The problem stems from the fact that, even with the wide range of ionizations that photoionization can produce, it is impossible to formulate a single-zone model with, for example, the N III and O IV lines forming in the same region as the N V and O VI lines. As might be expected, a two-zone model yields much better results, although being limited to two zones in certain models is somewhat unphysical and its acceptance might imply a wider range of actual ionization zones. In particular, models in which density fluctuations in individual clouds produce ionization stratification would be expected to have a range of intermediate densities. From photoionization calculations using G. Ferland's code CLOUDY and several different forms of ionizing continua (e.g., the AGN photoionizing continuum proposed by Mathews & Ferland 1987 and simple power laws with exponential high-energy cutoffs at ~ 0.3 keV, which is consistent with weak intrinsic X-ray emission in BAL QSOs), we have determined values for two ionization parameters (u_1, u_2) and the ratio of the thicknesses of the two zones along the sight line ($R \equiv \Delta r_1/\Delta r_2$) as being representative of cases that come close to matching the column density ratios and estimated errors that have been derived from the observations for N and O.

In making the selections of u_1, u_2, and R to match the observed column density ratios, we assumed, as noted earlier, that the observed ions were near their dominant stages. However, even with this constraint, it should be understood that variations in the values of u_1, u_2, and R near the deduced values may still be roughly consistent with the observed column density ratios. We have not bothered to determine the range of possible values of u_1, u_2, and R because of the dependence on photoionizing continuum shape, which is probably a greater uncertainty; however, we did make an attempt to fine-tune these values along with the abundances to match the observations and check for consistency in any finally adopted model. The results we report are adequate for exploring some of the properties that a successful two-zone photoionization model might possess. The results are shown in Table 3, where the reported value for R is in the context of a density fluctuation model (see below). The photoionization models were run for an electron density of $n_e \approx 10^8$ cm^{-3}, which is consistent with constraints found by Turnshek et al. (1985), and abundances near the deduced values (§ 5). No significant BAL-region He I or He II Lyman continuum opacity was included in the calculation. The H I Lyman continuum opacity is known to be very small, based on direct observation (e.g., this study and the H I column densities in Table 2). In principle, we would expect absorption from the BAL troughs themselves to be a definite source of opacity in the ionizing continuum, but this was also neglected because there is no evidence for *significant* ionization changes with outflow velocity (but see § 6, point 5).

As an example of our results and their interpretation, we discuss the results inferred from adopting the Mathews & Ferland (1987) AGN photoionizing continuum (hereafter "MF87-AGN"), which offers a formulation of a standard model to test, and a power law with exponent -1.5, which is a simple model that also fits the data reasonably well (somewhat better than the MF87-AGN model).

To obtain reasonable agreement with the Q0226−1024 column density ratios, the inferred ionization parameters for the two zones are $\log u_1 \approx -1.20$ and $\log u_2 \approx -2.70$ in the MF87-AGN model and $\log u_1 \approx -1.25$ and $\log u_2 \approx -2.45$ in the $\nu^{-1.5}$ model. For clouds in a single spatial region, the required ionization parameters suggest density fluctuations of ~ 32 and ~ 16 for the MF87-AGN and $\nu^{-1.5}$ ionizing continua, respectively. Again, we have not bothered to consider the range of values of u_1, u_2, and R that might adequately explain the data for a given photoionizing continuum since the uncertainty in continuum shape is probably the major uncertainty at this stage. However, for

© American Astronomical Society • Provided by the NASA Astrophysics Data System

1996ApJ...463..110T

TABLE 3

COMPARISON WITH CENTRAL-SOURCE PHOTOIONIZATION MODEL

			COMPUTED RATIOS[a]				
SPECIES RATIO	OBSERVED	ERROR	MF87-AGN $u_1 = -1.20$ $u_2 = -2.70$ $R = 60$[b]	Power Law, ν^{-1} $u_1 = -1.25$ $u_2 = -2.45$ $R = 19$[b]	Power Law, $\nu^{-1.5}$ $u_1 = -1.25$ $u_2 = -2.45$ $R = 27$[b]	Power Law, ν^{-2} $u_1 = -1.10$ $u_2 = -2.50$ $R = 38$[b]	Power Law, ν^{-3} $u_1 = -0.45$ $u_2 = -2.60$ $R = 250$[b]
$N(C^+)/N(C^{+2})$	< 0.64	< 0.1	0.13	0.08	0.09	0.12	0.27
$N(C^{+2})/N(C^{+3})$	0.25	0.05	0.75	0.81	0.70	0.88	0.84
$N(N^{+2})/N(N^{+3})$......	0.91	0.3	1.01	1.16	1.06	1.12	1.20
$N(N^{+3})/N(N^{+4})$......	1.00	0.2	0.88	1.18	0.93	1.04	0.88
$N(O^{+2})/N(O^{+3})$......	0.81	0.2	0.95	1.03	0.88	1.05	0.98
$N(O^{+3})/N(O^{+5})$......	1.80	0.4	3.10	1.00	1.54	3.07	4.45

[a] Calculated with CLOUDY version 84.09. Version 84.12a yields values of $N(C^{+2})/N(C^{+3})$ that are closer to ~ 1.2.

[b] $R \equiv \Delta r_1/\Delta r_2$, where R is reported in the framework of ionization parameter changes caused by density fluctuations.

such an absorbing region, these density fluctuations should be considered minimum values because there are only two zones and a two-zone cloud is unphysical. In such a model the absorbing region intersected by a sight line might consist of a denser inner region surrounded by (or trailed by) a less dense, more highly ionized outer region that has ~ 60 (MF87-AGN) to ~ 27 ($\nu^{-1.5}$) times the extent of that of the inner region. This could be a flattened geometry consistent with inferences from the Cloverleaf observations (Turnshek 1995; Turnshek et al. 1996), but in the manner suggested by Williams (1992) for incorporating density fluctuations into photoionization models. Figure 5*a* provides an illustration of such a case. However, other interpretations of the two-zone geometry are possible. Rather than density fluctuations, there may be two physically distinct regions, e.g., spatially well-separated from one another, with somewhat different but uniform densities and the same outflow velocities. Figure 5*b* provides an illustration of this case. In either case, both zones contribute significantly to the observed column densities. In the density fluctuation model, the lower density region must have a much larger extent along the sight line than the higher density region; this property allows it to contribute to the observed column densities despite its much lower density.

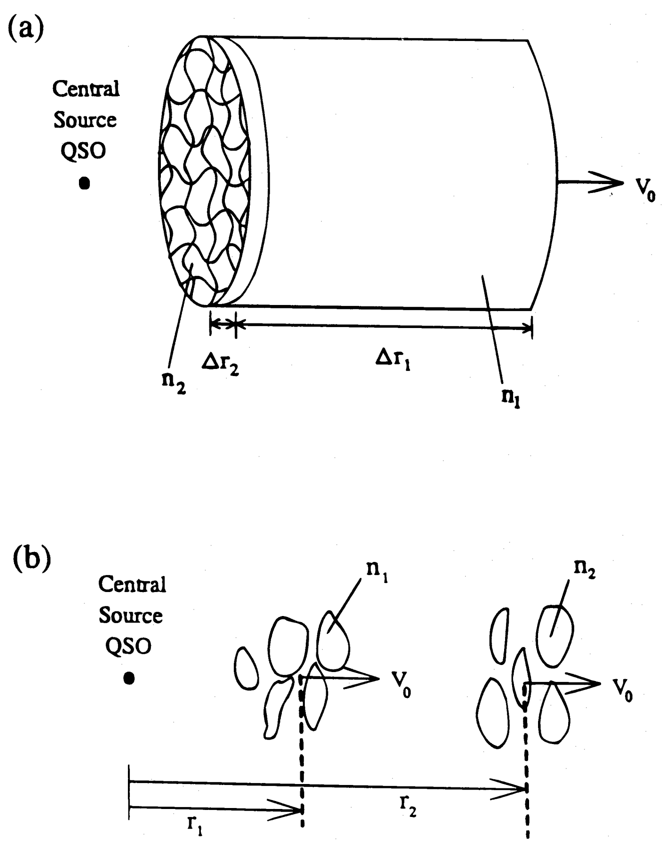

FIG. 5.—(*a*) Possible BAL cloud geometry for clouds at a specific outflow velocity, $v_{\rm outflow} = V_0$, in a photoionization model in which the two ionization zones are caused by density fluctuations. Here the density n_2 is $\sim$16–32 times larger than n_1, and $R \equiv \Delta r_1/\Delta r_2 \approx 27$–60. (*b*) Same as (*a*), but for a photoionization model in which the two ionization zones are spatially distinct and well separated in distance from the central source. If we assume that $n_2 \approx n_1$, then $(r_2/r_1)^2 \approx 16$–32. In this case, the thicknesses of the two absorbing zones at V_0, Δr_1 and Δr_2 (not labeled), are more similar in value, $R \equiv \Delta r_1/\Delta r_2 \approx 1.7$–1.9.

5. ELEMENTAL ABUNDANCES

Since a two-zone photoionization model comes close to matching the observed column densities, we consider the implications it raises for the elemental abundances of the BAL-region gas. We will describe how the various photoionization models that have been considered generally lead to the conclusion that the metal-to-hydrogen abundance ratios are very enhanced relative to solar values. Before continuing with this point, however, it should be noted that by adopting certain aspects of collisional ionization models, the requirements for large metal-to-hydrogen abundances could be severely reduced. For example, in a collisionally ionized zone with $\log T \approx 5$ (see § 4.1), the dominant ionization stages for C, N, and O will be C^{+2}, N^{+2}, and O^{+2}. In such a zone, the logarithm of the neutral hydrogen fraction is approximately -4.7, which is ~ 2 orders of magnitude lower than in the low-ionization zones, which produce most of the neutral hydrogen in our two-zone photoionization models. Thus, if collisional ionization were important, it would drastically lower our photoionization model estimates of metal-to-hydrogen abundances. On the other hand, results on the relative abundances of the metals are less dependent on the assumption of collisional ionization or photoionization because of the similar ionization potentials for the metals involved.

Once again, in the context of a two-zone photoionization model, we consider inferences that can be drawn by adopting an MF87-AGN or $\nu^{-1.5}$ ionizing continuum. As seen from Table 3, which presents results for various assumptions about the shape of the correct ionizing continuum, two-zone models explain the ratios of column densities of

© American Astronomical Society • Provided by the NASA Astrophysics Data System

1996ApJ...463..110T

different ions of the same element for both N and O with the same two ionization parameters. However, the abundances required for an acceptable fit to the metal BALs are very different from solar values. These results are reported in Table 4 for the various ionizing continua that have been investigated. Note that in Table 4 we have not bothered to give the abundances deduced from each of the C, N, and O ions separately. For N and O, the determinations are well within the observational errors and are therefore consistent, and the average is taken. On the other hand, there is a problem with C. The model we finally accepted has an $N(C^{+2})/N(C^{+3})$ ratio that is too large (Table 3), but this may be because there is some difficulty with obtaining an accurate prediction from the CLOUDY model (see Table 3, note a). The results for C should be considered less reliable.

For an MF87-AGN ionizing continuum, values of $(N/O) \approx 3(N/O)_{\odot}$ and $(N/C) \approx 10(N/C)_{\odot}$ (but with greater uncertainty) are necessary. A value $(N/H) \approx 230(N/H)_{\odot}$ is required to obtain an acceptable fit to the Lyα BAL. For a $\nu^{-1.5}$ ionizing continuum, $(N/O) \approx 4(N/O)_{\odot}$ and $(N/C) \approx 9(N/C)_{\odot}$ (still with greater uncertainty) are needed. However, in this case, $(N/H) \approx 120(N/H)_{\odot}$ is required to obtain an acceptable fit to the Lyα BAL. This is basically representative of a large N enhancement, with typically $(C/H) \approx (33\text{–}8)(C/H)_{\odot}$ for the models investigated.

Aside from C, N, and O, BALs due to other metals are seen in BAL QSOs. These include transitions due to Mg, Al, Si, P, S, and Fe. Among these metal BALs, there is also evidence for large enhancements. The Si IV transition is almost always observed in BAL QSOs, and in the Q0226−1024 BAL region we infer $(Si/H) \approx 82(Si/H)_{\odot}$ and $46(Si/H)_{\odot}$ for the MF87-AGN and $\nu^{-1.5}$ ionizing continua, respectively. Both S IV and S VI were also observed in Q0226−1024, and we infer $(S/H) \approx 180(S/H)_{\odot}$ and $130(S/H)_{\odot}$ for the MF87-AGN and $\nu^{-1.5}$ ionizing continua, respectively. An Ne VIII BAL is possibly present in the Q0226−1024 spectrum, but we do not consider it because of the difficulties in making a firm identification; in addition, while Ar VI seemed to be present, it was not accompanied by Ar V, so its existence is unclear. BALs due to Mg, Al, P, and Fe were too weak to detect with any certainty in the Q0226−1024 spectrum, but they have been detected in other objects.

There is clear evidence of enhancement of two of these rarer elements, P and Fe, in some objects. Given the optical depths inferred for the more common metal BALs due to C, N, and O, it would be unlikely to observe these rarer elements unless they were enhanced, sometimes well in excess of 100 times solar values relative to hydrogen in the framework of the photoionization models. Note that both the relevant P and Fe transitions, i.e., P V λλ1117, 1128 and Fe III λ1122, would produce absorption near a rest-frame wavelength of ~1122 Å. Turnshek et al. (1987) found it difficult to distinguish between P V and Fe III in the spectrum of H1413+1143, which nevertheless clearly shows S IV, S VI, and Al III BALs. However, some recent spectra indicate that there are a few clear cases in which the P V doublet separation is seen. For example, from an analysis of the BALs in the *HST* spectrum of PG 0946+301, Junkkarinen et al. (1995) have presented convincing evidence for a P V identification that would require $(P/C) \approx (60\text{–}80)(P/C)_{\odot}$. The P V identification in PG 0946+301 is bolstered by the presence of P IV. The P V transition also may be present in our *HST* FOS spectrum of H0059−2735 (see Fig. 1), however, we have not considered the possible presence of excited-state absorption. In this same object, Wampler et al. (1995) have discussed the identification of Fe II BALs from excited states.

There also is now evidence of dust in some BAL QSO spectra, mostly those that exhibit evidence of low-ionization BALs (Weymann et al. 1991; Sprayberry & Foltz 1992; but see also Turnshek et al. 1994 for a case in which there may be dust and no observable low-ionization BALs). Assuming that dust is present, it is not clear if it is mixed in with the BAL region.

Last, turning to the broad emission lines, their properties have also been cited as evidence of enhancements. This result is relevant if the BAL and broad emission line regions are physically related or connected (Lee & Turnshek 1995). For this work, the following should be noted: First, there is an energy-budget problem with Fe II emission in some QSOs (see Netzer 1990), and part of the solution is likely to rely on large (>10) enhancements of Fe relative to solar values. BAL QSOs as a class have enhanced Fe II emission (Weymann et al. 1991), and the recent study of the BAL QSO PG 0043+039 (Turnshek et al. 1994) shows it to be one of the strongest known Fe II emitters. Second, based on the N V/C IV and N V/He II broad emission line ratios in QSO spectra, Hamann & Ferland (1993) have argued that in some cases N must be enhanced relative to solar values. Accepting this result for the broad emission line region raises at least one interesting question in relation to the BAL-region results discussed here. In particular, given the strong N V BAL that is seen in all BAL QSO spectra, we suspect that enhanced N may be a universal phenomenon in the BAL region; however, N V emission is *not* systematically strong in all QSO spectra. Does this represent real variations in N abundances in broad emission line regions, or is

TABLE 4

DEDUCED ABUNDANCES FROM TWO-ZONE PHOTOIONIZATION MODELS

	Abundance (X/H) Relative to $(X/H)_{\odot}$				
Element	MF87-AGN $u_1 = -1.20$ $u_2 = -2.70$ $R = 60$	Power Law, ν^{-1} $u_1 = -1.25$ $u_2 = -2.45$ $R = 19$	Power Law, $\nu^{-1.5}$ $u_1 = -1.25$ $u_2 = -2.45$ $R = 27$	Power Law, ν^{-2} $u_1 = -1.10$ $u_2 = -2.50$ $R = 38$	Power Law, ν^{-3} $u_1 = -0.45$ $u_2 = -2.60$ $R = 250$
C[a]	22:	23:	14:	10:	8:
N........	230	210	120	120	89
O........	72	43	29	35	46
Si........	82	59	46	47	51
S	180	490	130	110	110

[a] Average from C^{+2} and C^{+3} column densities.

© American Astronomical Society • Provided by the NASA Astrophysics Data System

1996ApJ...463..110T

it the result of changes in physical conditions? It should also be noted that Hamann & Ferland did not take into account resonance-line scattering in the BAL region, which may enhance the N v broad emission line (Turnshek 1984a, 1988); however, the importance of such an effect is unclear, and it may be negligible (Hamann et al. 1993; Hamann & Korista 1996) or be destroyed by dust (see Turnshek et al. 1994).

In any case, results on abundances in the broad emission line region certainly have relevance to BAL-region abundance studies. For example, if it could be shown that the abundances in the two regions were the same or consistent, this would strengthen the evidence that the two regions are physically related. However, if the abundances were vastly different, it would be hard to imagine how the regions could be related.

6. THE NEED FOR FUTURE WORK AND SOME IMPLICATIONS

The results discussed here on ionization structure and elemental abundances need to be checked and improved upon in a number of ways:

1. The photoionization model analysis that has been performed indicates very high elemental abundances relative to hydrogen. This result primarily stems from the weakness of the Lyα BAL. Clearly, additional high-resolution studies of BAL profiles are needed to understand the limitations of column density derivations, especially in the region of the Lyα BAL.
2. Theoretical work is needed to explain the nature of the inferred ionization structure that gives rise to multiple ionization zones at the same observed outflow velocities.
3. There are no observational constraints that would demand that the ionizing continuum follow the one proposed by Mathews & Ferland (1987) or the more simple ones that we considered here. BAL QSOs may in fact have different continuum properties than non-BAL QSOs, as inferred from the fact that they seem to be X-ray–quiet. The dependences between the shape of the ionizing continuum, inferred ionization structure, and elemental abundances need to be considered in more detail. It is clear from Table 4 that the deduced metal-to-hydrogen abundance enhancement could be reduced if a steeper ionizing continuum were used near the hydrogen ionization edge (i.e., a blue bump) in the context of a multizone model, because then models could be constructed in which more hydrogen would be ionized relative to the metals. At the same time, models that incorporated collisionally ionized regions could also lower the deduced metal-to-hydrogen abundances even more drastically.
4. While the shape of the ionizing continuum and its nature may have a substantial effect on the elemental abundances relative to hydrogen, there is less of an effect on the deduced relative enhancements of the metals, because the metals have a similar range of ionization potential. For example, it seems clear that some mechanism of N/O and N/C enhancement relative to solar values is required.
5. The nature of the photoionization model itself, as applied to BAL column density modeling, needs to be better understood. For example, the effects that far-UV BAL profiles and the outflow velocity law would have on the shape of the photoionizing continuum and the effects of very enhanced abundances need to be considered more carefully. One large concern involves understanding why the ionization of a BAL trough often remains roughly constant as a function of outflow velocity despite the fact that the inner parts of the BAL outflow must absorb a substantial fraction of any ionizing photons from a central source. In a successful central-source photoionization model for the BAL region, it seems that the density of the BAL gas must drop by just the right amount to balance the loss of ionizing photons (due to absorption by BALs from the inner parts of the flow) and the change in central-source distance, keeping the ionization of the gas roughly constant with outflow velocity. Perhaps this is not a case of central-source photoionization.
6. Theoretical work is needed to explain the inferred abundance enhancements. Hamann & Ferland (1993) have discussed chemical evolution calculations that may be relevant to interpreting an inferred N enhancement. If normal stellar nucleosynthesis is important, their results indicate that a relatively flat initial mass function would be required so that an N overabundance could be produced by secondary processing in massive stars. However, the observation that elements like P are greatly enhanced in a (possibly small) fraction of the objects may provide clues that point to a more complicated enrichment scenario.
7. Observation and analysis in more QSOs of far-UV BAL profiles that include different ions of the same element are needed to check the reliability of these results and help isolate any systematics of abundance enhancements with other QSO properties.

7. SUMMARY

While absorption from BAL gas does not appear to be completely uniform across the continuum source along a sight line, the average absorption profile is clearly very similar across a region that exceeds the size of the continuum source and even the size of the Lyα broad emission line region. Thus, with few exceptions the BAL region probably completely covers the unpolarized central continuum source. We have therefore argued that the methods used to derive column densities are generally accurate enough in certain velocity intervals to perform an analysis of ionization structure and elemental abundances. Consequently, the work discussed here suggests the following main points:

1. A two-zone photoionization model with ionization parameter fluctuations of at least $\sim$32–16 is needed to obtain reasonable agreement with the observed column densities of different ions of the same element. This requirement might be caused by density fluctuations in individual clouds or in regions with possibly similar densities and outflow velocities but different locations, so the location of the ionization zones in this model is not currently well constrained.
2. Compared to solar values, general enhancements of N relative to O and C of $\sim$4–3 and $\sim$9:–10: times solar values, respectively, are needed. Deduced enhancements relative to hydrogen are very large, $(N/H) \approx (120\text{–}230)(N/H)_{\odot}$, but more model-dependent. The rarer elements S, P, and Fe also exhibit large enhancements in some BAL QSOs.
3. Ways to lessen the inferred metal enhancements relative to hydrogen include hypothesizing a multizone ionization model with an ionizing continuum shape that would ionize more of the hydrogen, hypothesizing the existence of

© American Astronomical Society • Provided by the NASA Astrophysics Data System

1996ApJ...463..110T

collisionally ionized regions, and/or hypothesizing some effect that would cause the neutral hydrogen column density to be underestimated based on analysis of the Lyα BAL profile. However, the result that N is enhanced relative to some other metals (e.g., O and C) is more robust.

4. The general enhancement of N suggests that if normal stellar nucleosynthesis is important, a relatively flat initial mass function is involved, with the N overabundance being produced by secondary processing in massive stars. On the other hand, the existence of very enhanced P and other metals in some objects probably indicates that a more complex enrichment scenario is involved.

5. More observational and theoretical work is needed, to develop a more self-consistent model for the ionization that does not suffer from the problems discussed in § 6. Detailed work on abundance enhancements and possible enrichment scenarios can follow.

We wish to thank F. Hamann, C. Hazard, J. Hillier, V. Khersonsky, K. Korista, and J. Wampler for helpful discussions during the course of this work and S. Sherer for assistance. We also wish to thank G. Ferland for the development of CLOUDY and his making it generally available. This work was based on observations made with the NASA/ESA *Hubble Space Telescope*, operated by AURA, Inc., under NASA contract NAS 5-26555.

REFERENCES

Arnaud, M., & Rothenflug, R. 1985, A&AS, 60, 425
Barlow, T. A. 1995, BAAS, 27, 872
Barlow, T. A., & Junkkarinen, V. T. 1994, BAAS, 26, 1339
Burbidge, E. M. 1995, in QSO Absorption Lines, ed. G. Meylan (Berlin: Springer), 201
Ferland, G. J., Peterson, B. M., Horne, K., Welsh, W. F., & Nahar, S. N. 1992, ApJ, 387, 95
Foltz, C. B., Weymann, R. J., Morris, S. L., & Turnshek, D. A. 1987, ApJ, 317, 450
Goodrich, R. W., & Miller, J. S. 1995, ApJ, 448, L73
Grillmair, C. J., & Turnshek, D. A. 1987, in QSO Absorption Lines: Probing the Universe (Poster Papers), ed. J. C. Blades, C. A. Norman, & D. A. Turnshek (Baltimore: STScI), 1
Hamann, F., & Ferland, G. J. 1993, ApJ, 418, 11
Hamann, F., & Korista, K. T. 1996, ApJ, in press
Hamann, F., Korista, K. T., & Morris, S. L. 1993, ApJ, 415, 541
Hazard, C., McMahon, R. G., Webb, J. K., & Morton, D. C. 1987, ApJ, 323, 263
Hazard, C., Morton, D. C., Terlevich, R., & McMahon, R. G. 1984, ApJ, 282, 33
Junkkarinen, V. T., Burbidge, E. M., & Smith, H. E. 1983, ApJ, 265, 51
Junkkarinen, V. T., et al. 1995, BAAS, 27, 872
Korista, K. T., Hamann, F., Ferguson, J., & Ferland, G. J. 1996, ApJ, 461, 641
Korista, K. T., et al. 1992, ApJ, 401, 529
Lee, L. W., & Turnshek, D. A. 1995, ApJ, 453, L61
Mathews, W. G., & Ferland, G. J. 1987, ApJ, 323, 456
Netzer, H. 1990, in Proc. Saas-Fée Adv. Course 20, Active Galactic Nuclei, ed. T. Courvoisier & T. Mayor (Berlin: Springer), 57
Shull, J. M., & Van Steenberg, M. 1982, ApJS, 48, 95; erratum 49, 351
Sprayberry, D., & Foltz, C. B. 1992, ApJ, 390, 39
Turnshek, D. A. 1984a, ApJ, 278, L87
———. 1984b, ApJ, 280, 51
———. 1988, in QSO Absorption Lines: Probing the Universe, ed. J. C. Blades, D. A. Turnshek, & C. A. Norman (Cambridge: Cambridge Univ. Press), 17
———. 1995, in QSO Absorption Lines, ed. G. Meylan (Berlin: Springer), 223
Turnshek, D. A., Briggs, F. H., Foltz, C. B., Grillmair, C. J., & Weymann, R. J. 1987, in QSO Absorption Lines: Probing the Universe (Poster Papers), ed. J. C. Blades, C. A. Norman, & D. A. Turnshek (Baltimore: STScI), 4
Turnshek, D. A., et al. 1994, ApJ, 428, 93
Turnshek, D. A., Foltz, C. B., Grillmair, C. J., & Weymann, R. J. 1988, ApJ, 325, 651
Turnshek, D. A., et al. 1996, in preparation
Turnshek, D. A., Weymann, R. J., Carswell, R. F., & Smith, M. G. 1984, ApJ, 278, 486
Turnshek, D. A., et al. 1985, ApJ, 294, L1
Wampler, E. J., Chugai, N. N., & Petitjean, P. 1995, ApJ, 443, 586
Weymann, R. J. 1995, in QSO Absorption Lines, ed. G. Meylan (Berlin: Springer), 213
Weymann, R. J., Morris, S. L., Foltz, C. B., & Hewett, P. C. 1991, ApJ, 373, 23
Williams, R. E. 1992, ApJ, 392, 99

© American Astronomical Society • Provided by the NASA Astrophysics Data System